nature climate change

ARTICLES

https://doi.org/10.1038/s41558-021-01223-2

# Climate and land-use changes reduce the benefits of terrestrial protected areas

Ernest F. Asamoah[1]✉, Linda J. Beaumont[2] and Joseph M. Maina[1]

**Expanding and enhancing protected area networks (PAs) is at the forefront of efforts to conserve and restore global biodiversity but climate change and habitat loss can interact synergistically to undermine the potential benefits of PAs. Targeting conservation, adaptation and mitigation efforts requires understanding climate and land-use patterns within PAs, both currently and under future scenarios. Here, projecting rates of temporal and spatial displacement of climate and land-use revealed that more than one-quarter of the world's PAs (~27%) are located in regions that will experience both high rates of climate change and land-use change by 2050. Substantial changes are expected to occur more often within PAs distributed across tropical moist and grassland biomes, which currently host diverse tetrapods and vascular plants, and fall into less-stringent management categories. Taken together, our findings can inform spatially adaptive natural resource management and actions to achieve sustainable development and biodiversity goals.**

Protected areas (PAs) are a fundamental tool for protecting Earth's biodiversity from excessive extinction rates and erosion of goods and services[1,2]—enhancing local biodiversity[3], water and soil retention, sandstorm prevention, carbon sequestration[4] and human well-being services[5]. Recent reporting indicates that households living near a PA are wealthier than those living far from PAs, providing empirical support for the livelihood benefits of PAs[5]. Despite the immense value of PAs, there is an ongoing debate on their overall effectiveness under global change[6], with recent evidence of mixed outcomes from the protection of avian species hotspots globally[7]. The continued decline of the positive role of PAs is expected to increase, given that climate conditions available for species within spatially static PAs will alter as climate change intensifies[8–10]. Moreover, habitat loss and fragmentation resulting from human activities are causing a structural disconnection across PA networks that impedes the ability of species to undergo range shifts and track their climate envelope[11–14]. Assessing the exposure risks of current PA networks into the future and the potential for the biodiversity they contain to respond to the combined impacts of these stressors is crucial to developing adaptive management approaches to conservation[15,16].

This paper examines spatiotemporal changes in climate and land use across biomes and within PAs globally. Using regionally downscaled temperature and precipitation data from the Coordinated Regional Climate Downscaling Experiment (CORDEX)[17] and moderate-resolution land-use states from the Harmonized Global Land Use (LUH2 v.2f) project[18], we present climate and land-use changes as a velocity ($km\,yr^{-1}$)—the ratio of temporal trends ($°C\,yr^{-1}$ or $\%\,yr^{-1}$) to the spatial gradient ($°C\,km^{-1}$ or $\%\,km^{-1}$). For both stressors, we consider estimates based on the representative concentration pathway RCP 8.5 or shared socioeconomic pathway SSP 5 and RCP 2.6 or SSP 1, which we refer to hereafter as SSP 585 and SSP 126, respectively.

Climate velocity, the rate and direction at which climate is moving, is a valuable surrogate for the potential movement requirements of species over time, as conditions across their range become less similar to the baseline epoch[19]. Likewise, land-use velocity (hereafter termed land-use instability) represents land-use composition changes across a spatially varying gradient[20]. We examine and compare climate velocity and land-use instability for the near future (2021–2050) and distant future (2071–2100) relative to the baseline of 1971–2000. Changes during the near future are particularly important as they may influence the achievement of the 2030 targets for sustainable development[21] and the Convention on Biological Diversity's 2050 biodiversity vision of 'living in harmony with nature'[22]. From this perspective, we examine correlations between climate velocity, land-use instability and characteristics of PAs such as native richness of tetrapods (that is, the richness of birds, mammals, reptiles and amphibians) and vascular plants, and PA location (that is, Euclidean distance from the ocean and elevation). We also examine differences in exposure of PAs under different management restrictions. Relating expected changes in environmental conditions within PAs can inform decisions to modify PAs to accommodate ecologically dynamic conservation objectives[23].

We find that the projected velocity at which a species may be required to track its climate envelope during the near future averages $3.1\,km\,yr^{-1}$ (interquartile range (IQR) = $4.3\,km\,yr^{-1}$) under the SSP 126 scenario and increases to $5.4\,km\,yr^{-1}$ (IQR = $7.1\,km\,yr^{-1}$) under the SSP 585 scenario (Supplementary Table 1). Climate velocity over the latter scenario was ~140% higher than the median dispersal velocity of 493 non-volant mammals (median = $1.4\,km\,yr^{-1}$; ref. [24]) and ~120% higher than the median poleward migration rates of bird, insect and mammal species (median = $16.9\,km\,decade^{-1}$; ref. [25]). Further, a strong positive correlation exists between climate velocity computed for the SSP 585 and SSP 126 scenarios (bivariate regression: coefficient of determination $r^2 = 0.77$; Fig. 1a,c). The positive association suggests that areas on the globe where species are likely to benefit from reduced climate change under SSP 126 are also areas projected to experience the highest climate change under SSP 585. However, the magnitude of velocity varies across bioregions (Fig. 1b). Given that the current global warming trajectory more closely aligns with SSP 585 (ref. [26]), we focus on the dynamics projected under this scenario.

[1]Department of Earth and Environmental Sciences, Macquarie University, Sydney, New South Wales, Australia. [2]Department of Biological Sciences, Macquarie University, Sydney, New South Wales, Australia. ✉e-mail: asamfrt@gmail.com

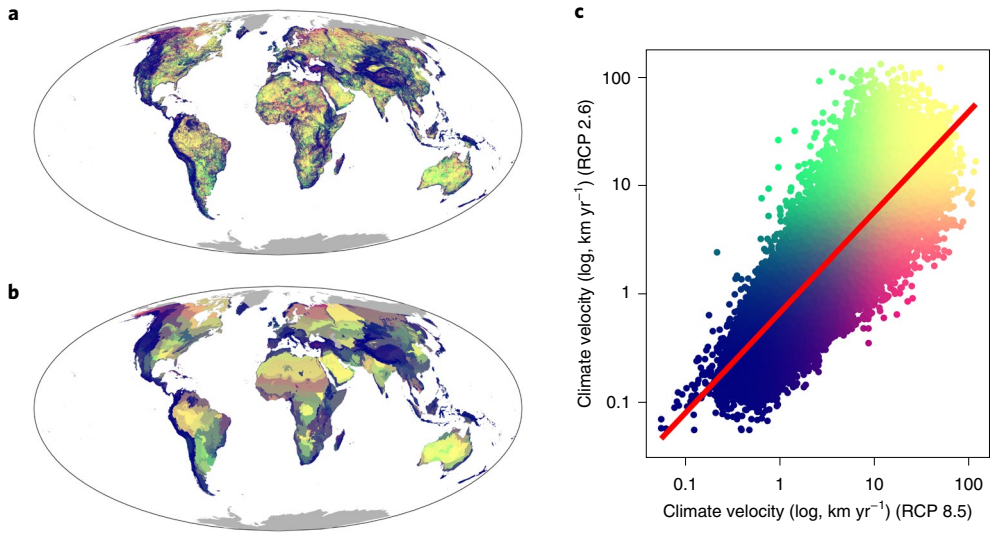


**Fig. 1 | Spatial concordance of climate velocity projected under the RCP 8.5 and RCP 2.6 scenarios. a**,**b**, Maps show spatial congruence of SSP 585 and SSP 126 at pixel (**a**) and ecoregional (**b**) scales. **c**, Bivariate linear regression: $\log(Y) = 0.92 \times \log(X) - 0.38$, $r^2 = 0.77$, $P \leq 1.0 \times 10^6$, $N_{cells} = 218{,}528$. Climate change results are based on the final projections at a spatial resolution of 24 km in a Mollweide projection (ESRI: 54009). Grey regions of the terrestrial surface were excluded from our analysis (see 'Climate and land-use data' subsection for details).

**Table 1 | Summary of climate velocity and land-use instability globally and within PAs**

| | 1971–2000 | | 2021–2050 | | 2071–2100 | | $N_{cells}$ |
|---|---|---|---|---|---|---|---|
| | Median | IQR | Median | IQR | Median | IQR | |
| Climate velocity (km yr$^{-1}$) | | | | | | | |
| Global median | 3.6 | 5.1 | 5.4 | 7.1 | 7.4 | 10 | 218,528 |
| Protected | 3.0 | 5.0 | 4.7 | 7.0 | 6.5 | 11 | 29,345 |
| • I–II | 2.5 | 4.4 | 4.1 | 6.6 | 5.5 | 10 | 6,174 |
| • III–NA | 3.2 | 5.1 | 4.9 | 7.2 | 6.8 | 11 | 23,171 |
| Unprotected | 3.7 | 5.1 | 5.6 | 7.1 | 7.5 | 9.8 | 187,286 |
| Land-use instability (km yr$^{-1}$) | | | | | | | |
| Global median | 0.73 | 2.4 | 0.13 | 1.2 | 0.040 | 0.34 | 218,528 |
| Protected | 0.25 | 1.6 | 0.18 | 1.9 | 0.036 | 0.37 | 29,345 |
| • I–II | 0.041 | 0.74 | 0.23 | 2.0 | 0.029 | 0.21 | 6,174 |
| • III–NA | 0.34 | 1.8 | 0.16 | 1.8 | 0.036 | 0.40 | 23,171 |
| Unprotected | 0.83 | 2.5 | 0.13 | 1.1 | 0.040 | 0.34 | 187,286 |

Median and IQR for the near future (2021–2050) and distant future (2071–2100) are based on the SSP 585 scenario. 'Protected' refers to their International Union for Conservation of Nature (IUCN) management category: I–II have stricter conservation management objectives; III–NA either have less-stringent objectives (III–VI) or their status is depicted as 'Not Assigned', 'Not Reported' or 'Not Applicable' in the 2021 WPDA datasets. 'Unprotected' refers to all other areas outside protected pixels (Supplementary Fig. 1).

## Climate velocity and land-use instability in PAs

Within PAs, median climate velocity was 3.0 km yr$^{-1}$ (IQR = 5.0 km yr$^{-1}$) during the baseline epoch (1971–2000), which is slightly lower than the global median (median = 3.6 km yr$^{-1}$; IQR = 5.1 km yr$^{-1}$; Table 1) but increases to 4.7 km yr$^{-1}$ (IQR = 7.0 km yr$^{-1}$) during the near future. As the century progresses, velocity is projected to increase 32% to a median speed of 6.5 km yr$^{-1}$ (IQR = 11 km yr$^{-1}$) across PAs during the distant future. While velocity is consistently slowest in montane grasslands and shrublands, and coniferous forests, median rates above 5 km yr$^{-1}$ are projected across seven biomes by the distant future, reaching up to 12 km yr$^{-1}$ (IQR = 14 km yr$^{-1}$) in flooded grasslands and savannahs (Supplementary Table 2). Close examination of both future epochs shows that temperature velocity is faster than precipitation, with a median difference of 3.0 and 4.3 km yr$^{-1}$, respectively (Supplementary Table 1). These differences are predictable because the changes in precipitation over time tend to be lower than the spatial gradients. Moreover, both climate variables are weakly positively correlated (Spearman rho $|\rho| = 0.44$, $P \leq 1.0 \times 10^6$; $N_{cells} = 218{,}528$; Supplementary Fig. 2), suggesting spatial congruence in temperature and precipitation velocities.

We assess the effects of cumulative human pressure on the velocity at which species may be required to track suitable climate envelopes. To achieve this, we calculated land-use instability, with constraints on ten land-use facets projected under the SSP 585 scenario. In contrast to climate velocity, as the twenty-first century progresses, land-use instability is projected to decline under this scenario (Fig. 2). Instability for the near future was 0.18 km yr$^{-1}$ (IQR = 1.9 km yr$^{-1}$) across PAs, a decline of ~34% from the 1971–2000 baseline (median = 0.25 km yr$^{-1}$; IQR = 1.5 km yr$^{-1}$),

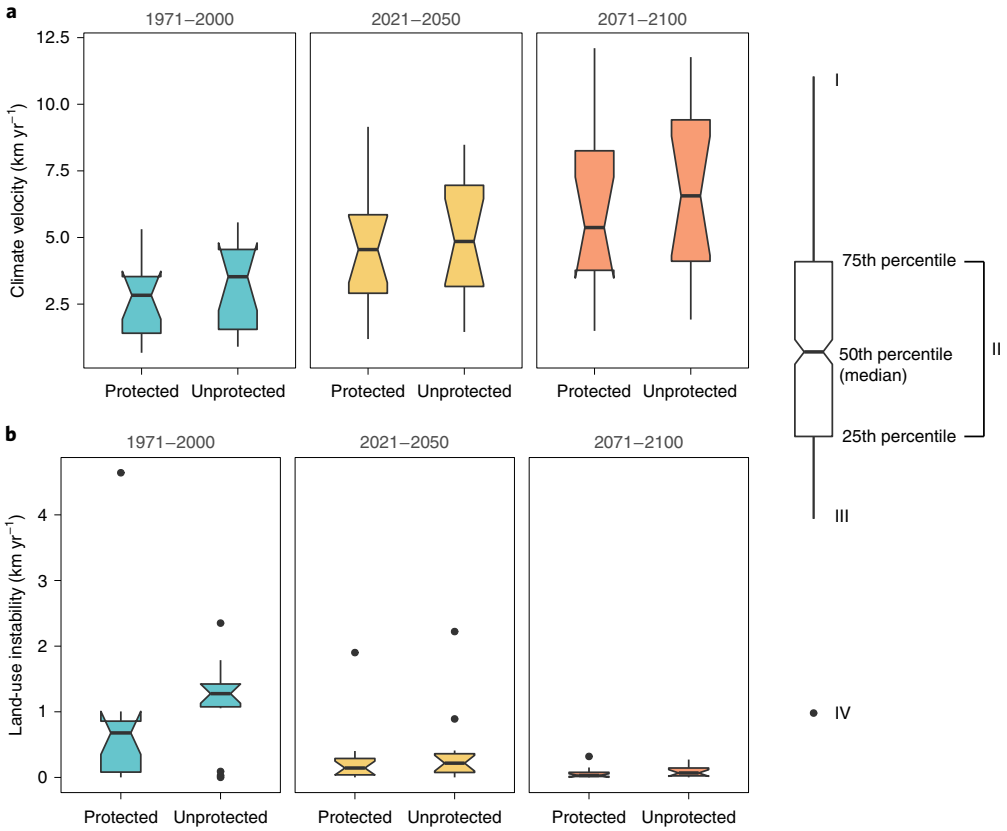


**Fig. 2 | Spatiotemporal distribution of climate velocity and land-use instability within terrestrial PAs globally. a**,**b**, Distribution of climate velocity (**a**) and land-use instability (**b**) for the baseline (1971–2000), near future (2021–2050) and distant future (2071–2100). Estimates for the near and distant future periods are based on the SSP 585 scenario. I and III, largest or smallest value within 1.5× IQR above 75th percentile or below 25th percentile; II and IV, >1.5× and <3× the IQR beyond either end of the box. Notched boxes indicate a 95% confidence interval of the median.

with values across biomes ranging between 0.01 and 1.9 km yr$^{-1}$ (Supplementary Table 2). During the near future, land-use instability is projected to be highest in protected tropical moist forests and tropical grassland and savannahs and lowest in temperate and desert and xeric biomes. However, by the century's end, instability could be greatest in taiga and boreal forests, although still considerably slower than previous epochs. The declining land-use instability suggests that much of the land-use transition from natural to human-modified forms with low transition potential may have already occurred by mid-to-late century, thus reducing the probability of spatial displacement of land use relative to small temporal trends in the future.

## Climate and land-use changes offset conservation gains

Mapping climate velocity and land-use instability together highlights opportunities for adaptation and conservation prioritization globally (Fig. 3). The intersection of the bivariate velocity space with PA locations suggests that the current arrangement of PAs and the spread across the exposure space represents a diversified portfolio, which can reduce environmental change-related conservation uncertainty[27]. We observed that 64% of PAs are poised to experience high rates of climate change by 2050 (percentage of evaluated protected cells, quadrants TL and TR; Fig. 3b). Most of these PAs (~37%) are located in regions where the velocity of expanding analogous climate may control environmental change within PAs relative to low land-use change.

In contrast, ~27% fall within regions where land-use instability is also high, suggesting that more than one-quarter of the current global investment in biodiversity conservation hedges towards high-risk zones during the near future. Locations of these PAs are concentrated in western and central Africa, northern North America, Amazonian South America and Southeast Asia (Fig. 3a). A lower percentage of PAs (17%) is projected to experience moderate climate velocity and land-use change (Fig. 3b; quadrant BL). These PAs are densely spread across montane regions of western North America and southern Andes of South America.

To explore these exposure spaces within the global conservation and sustainable development discourse, we examined associations of projected velocity and instability during the near future to key attributes of PAs—their management categories, location (elevation and distance from coasts) and species richness (native richness of birds, mammals, reptiles, amphibians and vascular plants) (Supplementary Figs. 3 and 4). We found PAs with higher levels of restrictions (IUCN PA categories I–II) to have lower climate velocity (Welch $t = P > 1.0 \times 10^6$) and similar land-use instability compared to other classifications (III–NA) (Supplementary Fig. 3). PAs with the fastest climate velocities were located near coasts and on relatively flat landscapes, suggesting species in coastal regions may need to move rapidly towards currently cooler regions to track their climate envelope[28], with a minimal topographical impediment to migration[29]. However, in contrast to climate, land-use instability across PAs generally increases rapidly towards the coast, indicating that projected coastal development may impede climate-driven range shifts in the near future. We also found a weak positive association between climate velocity and species richness, which markedly differed by biome and taxa, suggesting fundamentally different

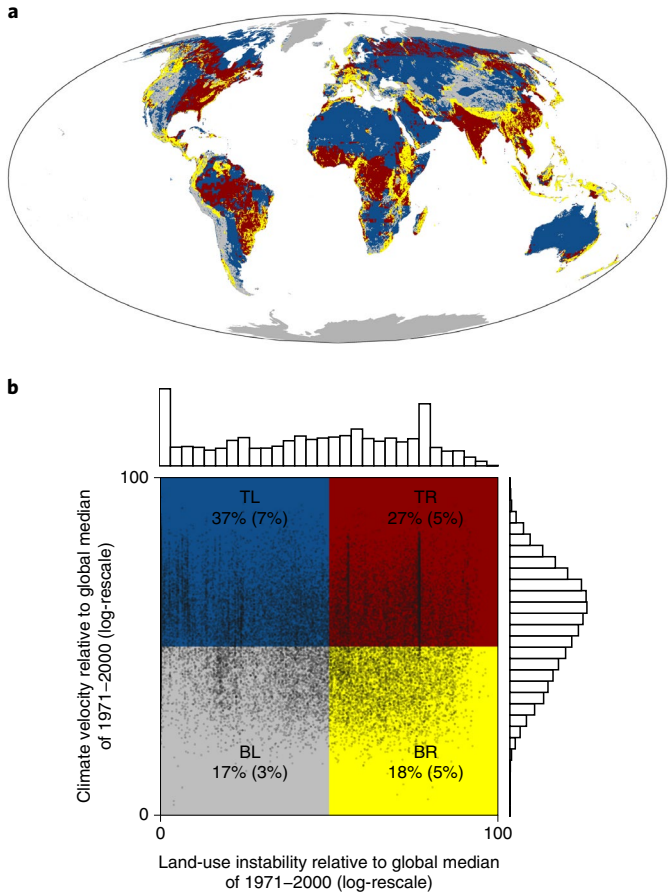


**Fig. 3 | Global patterns of climate velocity and land-use instability.** **a**, Bivariate choropleth map of climate velocity and land-use instability showing two-dimensional exposure space across the globe. Both metrics are calculated for the SSP 585 scenario across the near future (2021–2050) and presented as changes relative to the global median during the baseline epoch (1971–2000). **b**, Position of terrestrial PAs within the global climate velocity and land-use instability space. BL, slow-moving climate and stable land use (grey shades); TL, fast-moving climate and stable land use (blue shades); TR, fast-moving climate and rapidly changing land use (red shades); BR, slow-moving climate and rapidly changing land use (yellow shades). Numbers within brackets of respective quadrants correspond to PA pixels within each quadrant for strict IUCN categories. A *t*-test modified for spatial autocorrelations[44] showed a weak negative association between climate velocity and land-use change within PAs (coefficient = −0.11, $P = 4.0 \times 10^4$, $N_{cells} = 29{,}345$). Both climate and land-use change results are based on a spatial resolution of 24 km in a Mollweide projection (ESRI: 54009). Grey regions of the terrestrial surface were excluded from our analysis (see 'Climate and land-use data' subsection for details).

ecological and management consequences at multiple scales. Another reporting has suggested that PAs that are very important for conserving Red List species may be less affected by novel climate conditions until 2070 than relatively less important PAs[9].

## Ecological and policy implications

Here we harness moderate-resolution climate and land-use datasets in developing a metric at a global scale representing the speed at which species must migrate to keep pace with a shifting climate and the degree of land-use (in)stability they may face. Using these metrics, we examine the exposure risks of the current protected area networks into the future. Our results are affected by limitations stemming from data processing methods and data coverage. For example, assigning smaller and elongated polygons to ~24 km grid and omitting those designated as points may underestimate climate and land-use exposure risks for biodiversity residing within these PAs. We recognize that inadequate data across the Arctic region mean our analysis omits portions of the Arctic regions, which may experience erratic precipitation projected under 1.5 and 2.0 °C global warming[30]. Acknowledging these limitations, our study reveals notable climate change across PA locations showing similar patterns to those for unprotected areas (across all epochs). Results presented here concur with recent evidence indicating that accelerated global warming may alter conditions available for species in the spatially static PAs[8–10] and constrain the achievement of global biodiversity conservation goals. Moreover, we also show that land-use change might reinforce climate stress, albeit for some areas, revealing complementary and spatially adaptive management for spatially varying ecological consequences of global environmental change.

Importantly, our results indicate that one-third (~35%; Fig. 3b, quadrants BL and BR) of PAs may experience low rates of climate change by the mid-twenty-first century. Low-velocity regions may coincide with those where local climate conditions are less likely to shift[31]. Conversely, the relative likelihood that species assemblages will disaggregate in these areas may be low[32] and the slower velocity may facilitate biological responses such as migration or adaptive evolutionary change[32–34]. Worryingly, more than half of these PAs (~18%) are located in regions where land-use instability may be high, suggesting that land-use change may undermine putative climate refugia for species throughout eastern Europe, Scandinavia, eastern North America, Southeast Asia and eastern Africa (Fig. 3a and Extended Data Fig. 1a–c). Human-mediated reduction in vegetation integrity and structural connectivity often coincides with regions where climate stability may support species adaptation[15]. Therefore, localized land-use actions—such as expanding reserve systems, enhancing and protecting elevational gradients and intensive management—may benefit biodiversity and ecosystem services, in addition to global efforts to stabilize temperatures at or below 2 °C (refs. [35–37]).

Prioritization of protection, restoration and connectivity for PAs in those regions where our results suggest that the velocity of climate change is high may benefit some species by facilitating their connection to areas with analogous climate. However, given that for many species the velocity of change is likely to far exceed their dispersal capabilities (for example, >84% of non-volant mammals have dispersal velocities lower than the average climate velocity estimated by 2050[24]), other actions (including intensive management and the more controversial idea of managed translocation[35–37]) to promote tolerance or adaptation to climate change may be vital to their survival. To contextualize this in terms of policy, the restoration of about 350 million hectares of degraded land by 2030, as per the UN declaration of 'a Decade on Ecosystem Restoration', may benefit regions exposed to slow climate velocity and high land-use instability, such as the African Sahel, western North America, southern Latin America and northwest Asia. Therefore, it is important that policymakers define desired outcomes clearly and spatially target interventions accordingly. Initiatives aimed at establishing corridors would benefit from incorporating species- and biome-specific information to accommodate the marked discrepancies in land use and climate change across biomes (Fig. 4 and Supplementary Fig. 4). Conversely, efforts to enhance adaptation will be required for most regions, such as the eastern United States and European Union, where climate change may be the dominant driver of environmental change towards 2100.

The finding that more than one-quarter (27%) of PAs is projected to experience high climate velocity and high land-use change reinforces previous reports indicating that species' dispersal and survival may lag behind a highly unstable climate environment if change continues unabated[19,28,38,39]. Rapid changes to the use of landscapes may further impede the ability of species to spatially track movements of their climate niche[20,32,34], increasing extinction

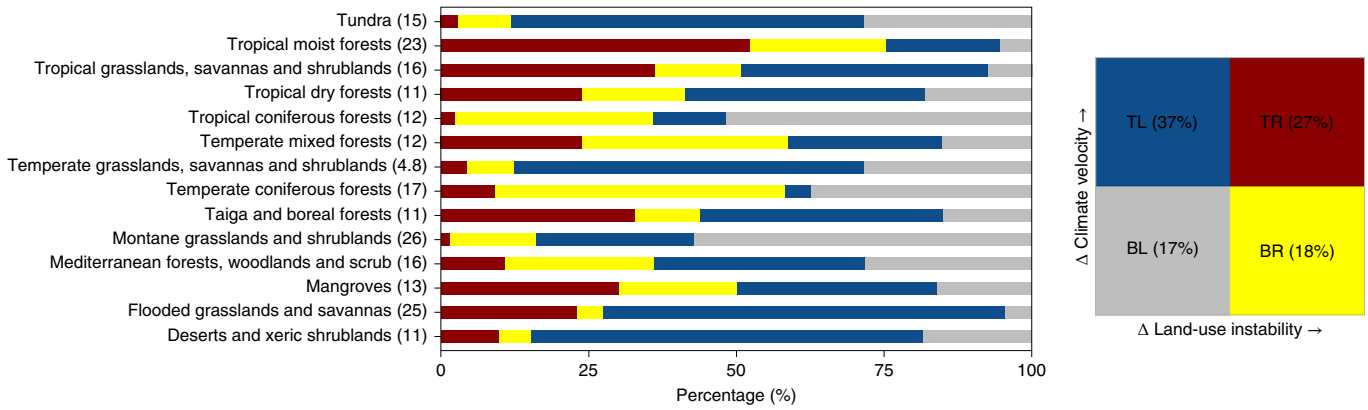


**Fig. 4 | Distribution of climate velocity and land-use change within PAs across terrestrial biomes during the near future (2021–2050) relative to a global median during the baseline (1971–2000).** BL, slow-moving climate and stable land use (grey shades); TL, fast-moving climate and stable land use (blue shades); TR, fast-moving climate and rapidly changing land use (red shades); BR, slow-moving climate and rapidly changing land use (yellow shades). Values within brackets of each quadrant correspond to the percentage of the evaluated protected cells. Values attached to biomes are the percentage of biomes protected.

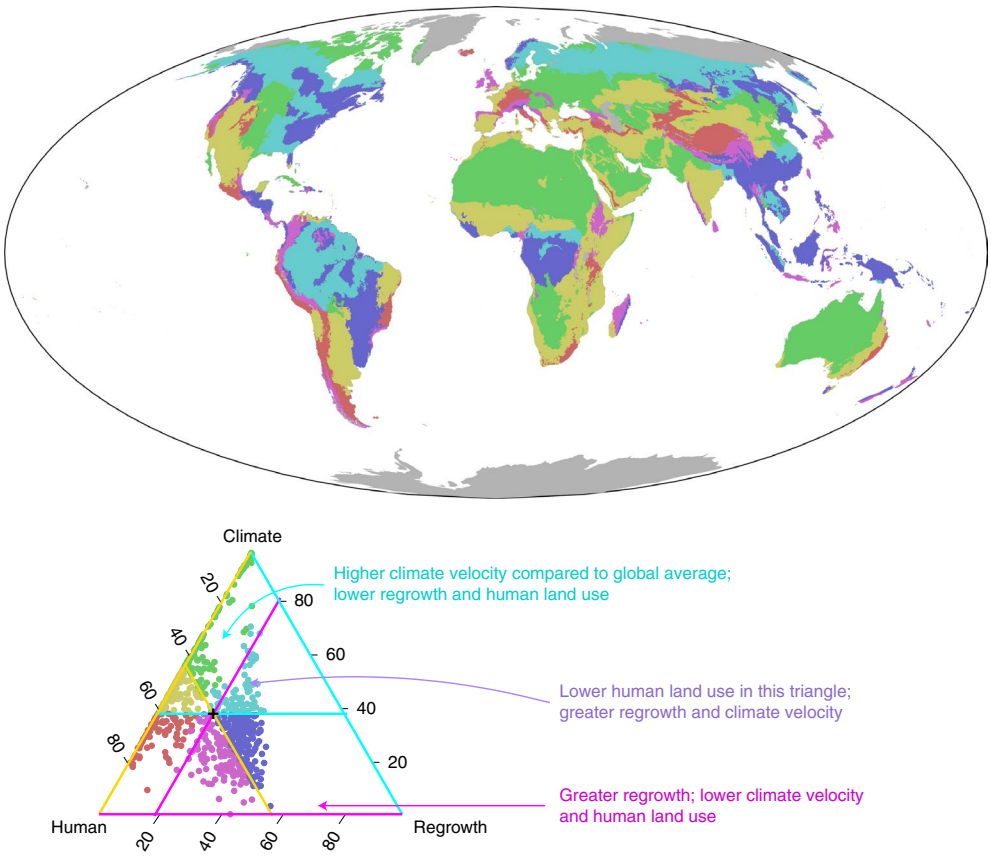


**Fig. 5 | Climate, human-dominated landscapes and forest growth potential during the 2021–2050.** The ternary scheme shows the intersection of climate (climate velocity), human-dominated landscapes (forest, cropland, urban and pasture instabilities) and regrowth (secondary forest instability) computed for the SSP 585 scenario. All three variables show deviations from the global mean (%). The plus sign (+) of the ternary legend shows the intersection of the global means of the three metrics (human (gold highlights), 43%; climate (cyan highlights), 38%; and regrowth (magenta highlights), 19%).

risks[40,41]—with resident species with low dispersal abilities being most vulnerable. These findings support the current view that future land-use change will compound climate stress, thereby seriously challenging global conservation goals[8,12,42]. While this may be the case, several evolving initiatives are looking beyond 2020. For example, the post-2020 framework of the Convention on Biological Diversity looks to embrace the 'reducing threats' goals of previous frameworks. To fully capture these goals, targets must be ambitious and measurable across all aspects of what makes PAs effective[42], including improved governance, targeted interventions and clear management plans[6]. Additionally, there is a need for explicit integration of climate adaptation principles into PA distribution and objectives to maintain network effectiveness as climate and land-use change[43].

So far, our analyses have focused on instabilities across all major land-use types (Methods). We recognize that not all land-use transitions will have negative consequences for biodiversity. Some land-use changes may favour species conservation and potential restoration of natural communities—for example, increases in forest cover[20]. Assessment of climate, human-dominated land-use and secondary forest concurrently showed general patterns that suggested that the regrowth of secondary forests following agricultural abandonment and other land management activities may compensate for and enhance a range of ecosystem services worldwide (Fig. 5). However, given that land-use instability declines towards 2100 (Fig. 2b) and human-dominated change could far exceed forest regrowth, land-use transition to natural forms would need to be at speed comparable to that of the baseline epoch for restoration and land management efforts towards reversing biodiversity decline to become effective. There are important exceptions, such as the Canadian boreal forests, Northern Russia, Scandinavia (for example, Norway) and Brazilian Amazon, where forest regrowth might be substantial by 2050. Nonetheless, further studies aimed at isolating the net transition velocities are required.

Despite the many complexities and limitations inherent in large-scale studies, our study offers a global quantitative synthesis that shows how climate and land use might interact to influence the dispersal and survival of species in the near term. Our results highlight biogeographic differences and the potential effectiveness of area-based management. Therefore, ambitious climate change mitigation that exploits synergies with land-use systems is required. Anticipating the effects of widespread climate and land-use changes on terrestrial ecosystems is crucial to developing adaptive management systems.

## Online content

Any methods, additional references, Nature Research reporting summaries, source data, extended data, supplementary information, acknowledgements, peer review information; details of author contributions and competing interests; and statements of data and code availability are available at https://doi.org/10.1038/s41558-021-01223-2.

Received: 23 February 2021; Accepted: 19 October 2021;
Published online: 25 November 2021

## References

1. Watson, J. E. M., Dudley, N., Segan, D. B. & Hockings, M. The performance and potential of protected areas. *Nature* **515**, 67–73 (2014).
2. Juffe-Bignoli, D. et al. *Protected Planet Report 2014* (UNEP-WCMC, 2014).
3. Gray, C. L. et al. Local biodiversity is higher inside than outside terrestrial protected areas worldwide. *Nat. Commun.* **7**, 12306 (2016).
4. Xu, W. et al. Strengthening protected areas for biodiversity and ecosystem services in China. *Proc. Natl Acad. Sci. USA* **114**, 1601–1606 (2017).
5. Naidoo, R. et al. Evaluating the impacts of protected areas on human well-being across the developing world. *Sci. Adv.* **5**, eaav3006 (2019).
6. Geldmann, J. et al. Effectiveness of terrestrial protected areas in reducing habitat loss and population declines. *Biol. Conserv.* **161**, 230–238 (2013).
7. Cazalis, V. et al. Effectiveness of protected areas in conserving tropical forest birds. *Nat. Commun.* **11**, 4461 (2020).
8. Elsen, P. R., Monahan, W. B., Dougherty, E. R. & Merenlender, A. M. Keeping pace with climate change in global terrestrial protected areas. *Sci. Adv.* **6**, eaay0814 (2020).
9. Hoffmann, S., Irl, S. D. H. & Beierkuhnlein, C. Predicted climate shifts within terrestrial protected areas worldwide. *Nat. Commun.* **10**, 4787 (2019).
10. Batllori, E., Parisien, M. A., Parks, S. A., Moritz, M. A. & Miller, C. Potential relocation of climatic environments suggests high rates of climate displacement within the North American protection network. *Glob. Change Biol.* **23**, 3219–3230 (2017).
11. Ward, M. et al. Just ten percent of the global terrestrial protected area network is structurally connected via intact land. *Nat. Commun.* **11**, 4563 (2020).
12. Jones, K. R. et al. One-third of global protected land is under intense human pressure. *Science* **360**, 788–791 (2018).
13. Parks, S. A., Carroll, C., Dobrowski, S. Z. & Allred, B. W. Human land uses reduce climate connectivity across North America. *Glob. Change Biol.* **26**, 2944–2955 (2020).
14. McGuire, J. L., Lawler, J. J., McRae, B. H., Nuñez, T. A. & Theobald, D. M. Achieving climate connectivity in a fragmented landscape. *Proc. Natl Acad. Sci. USA* **113**, 7195–7200 (2016).
15. Watson, J. E. M., Iwamura, T. & Butt, N. Mapping vulnerability and conservation adaptation strategies under climate change. *Nat. Clim. Change* **3**, 989–994 (2013).
16. Pecl, G. T. et al. Biodiversity redistribution under climate change: impacts on ecosystems and human well-being. *Science* **355**, eaai9214 (2017).
17. Jones, C., Giorgi, F. & Asrar, G. The coordinated regional downscaling experiment: CORDEX–an international downscaling link to CMIP5. *CLIVAR Exch.* **16**, 34–40 (2011).
18. Hurtt, G. C. et al. Harmonization of global land-use change and management for the period 850-2100 (LUH2) for CMIP6. *Geosci. Model Dev.* **13**, 5425–5464 (2020).
19. Loarie, S. R. et al. The velocity of climate change. *Nature* **462**, 1052–1055 (2009).
20. Ordonez, A., Martinuzzi, S., Radeloff, V. C. & Williams, J. W. Combined speeds of climate and land-use change of the conterminous US until 2050. *Nat. Clim. Change* **4**, 811–816 (2014).
21. *UN General Assembly Resolution A/RES/70/1* (UN, 2015).
22. Harrop, S. R. 'Living in harmony with nature'? Outcomes of the 2010 Nagoya conference of the convention on biological diversity. *J. Environ. Law* **23**, 117–128 (2011).
23. Maxwell, S. L. et al. Area-based conservation in the twenty-first century. *Nature* **586**, 217–227 (2020).
24. Schloss, C. A., Nuñez, T. A. & Lawler, J. J. Dispersal will limit ability of mammals to track climate change in the Western Hemisphere. *Proc. Natl Acad. Sci. USA* **109**, 8606–8611 (2012).
25. Chen, I. C., Hill, J. K., Ohlemüller, R., Roy, D. B. & Thomas, C. D. Rapid range shifts of species associated with high levels of climate warming. *Science* **333**, 1024–1026 (2011).
26. Schwalm, C. R., Glendon, S. & Duffy, P. B. RCP8.5 tracks cumulative $CO_2$ emissions. *Proc. Natl Acad. Sci. USA* **117**, 19656–19657 (2020).
27. Ando, A. W. & Mallory, M. L. Optimal portfolio design to reduce climate-related conservation uncertainty in the Prairie Pothole Region. *Proc. Natl Acad. Sci. USA* **109**, 6484–6489 (2012).
28. Ackerly, D. D. et al. The geography of climate change: implications for conservation biogeography. *Divers. Distrib.* **16**, 476–487 (2010).
29. Dobrowski, S. Z. & Parks, S. A. Climate change velocity underestimates climate change exposure in mountainous regions. *Nat. Commun.* **7**, 12349 (2016).
30. Hoegh-Guldberg, O. et al. in *Special Report on Global Warming of 1.5°C* (eds Masson-Delmotte, V. et al.) 175–311 (IPCC, WMO, 2018).
31. Sandel, B. et al. The influence of late Quaternary climate-change velocity on species endemism. *Science* **334**, 660–664 (2011).
32. Ordonez, A., Williams, J. W. & Svenning, J.-C. Mapping climatic mechanisms likely to favour the emergence of novel communities. *Nat. Clim. Change* **6**, 1104–1109 (2016).
33. Carroll, C. et al. Scale-dependent complementarity of climatic velocity and environmental diversity for identifying priority areas for conservation under climate change. *Glob. Change Biol.* **23**, 4508–4520 (2017).
34. Alexander, J. M. et al. Lags in the response of mountain plant communities to climate change. *Glob. Change Biol.* **24**, 563–579 (2018).
35. Lawler, J. J. et al. Projected land-use change impacts on ecosystem services in the United States. *Proc. Natl Acad. Sci. USA* **111**, 7492–7497 (2014).
36. Stein, B. A. et al. Preparing for and managing change: climate adaptation for biodiversity and ecosystems. *Front. Ecol. Environ.* **11**, 502–510 (2013).
37. Elsen, P. R., Monahan, W. B. & Merenlender, A. M. Global patterns of protection of elevational gradients in mountain ranges. *Proc. Natl Acad. Sci. USA* **115**, 6004–6009 (2018).
38. Burrows, M. T. et al. The pace of shifting climate in marine and terrestrial ecosystems. *Science* **334**, 652–655 (2011).
39. Burrows, M. T. et al. Geographical limits to species-range shifts are suggested by climate velocity. *Nature* **507**, 492–495 (2014).
40. Fitzpatrick, M. C., Gove, A. D., Sanders, N. & Dunn, R. R. Climate change, plant migration, and range collapse in a global biodiversity hotspot: the Banksia (Proteaceae) of Western Australia. *Glob. Change Biol.* **14**, 1337–1352 (2008).
41. Dynesius, M. & Jansson, R. Evolutionary consequences of changes in species' geographical distributions driven by Milankovitch climate oscillations. *Proc. Natl Acad. Sci. USA* **97**, 9115–9120 (2000).
42. Geldmann, J., Manica, A., Burgess, N. D., Coad, L. & Balmford, A. A global-level assessment of the effectiveness of protected areas at resisting anthropogenic pressures. *Proc. Natl Acad. Sci. USA* **116**, 23209–23215 (2019).
43. Tittensor, D. P. et al. Integrating climate adaptation and biodiversity conservation in the global ocean. *Sci. Adv.* **5**, eaay9969 (2019).
44. Osorio, F., Vallejos, R. & Cuevas, F. SpatialPack: Package for Analysis of Spatial Data. R package version 0.2-3 (2014).

## Methods

We aim to examine the potential changes in climate and land use within PAs to inform strategic investment in area-based measures for biodiversity conservation under climate change. Here, we describe the steps of our analysis from spatial-data collection to velocity of change calculations and risk assessments.

**Climate and land-use data.** We calculated climate velocity for contemporary baseline (1971–2000), near- (2021–2050) and distant-future (2071–2100) epochs on the basis of mean annual temperature and total annual precipitation. Temperature and precipitation data for past and future epochs were part of CORDEX of the Coupled Model Intercomparison Project Phase 5 (CMIP5). To reduce uncertainties inherent in projected data, we use three global circulation models (GCMs), MOHC-HadGEM2-ES[45], MPI-M-MPI-ESM-LR[46] and NCC-NorESM1-M[47]. These GCMs, downscaled by the GERICS-REMO2015 (v.1) regional climate model at ~0.22° spatial resolution (~24 km at the equator), were the only GCMs consistently available across all ten CORDEX regions. Additionally, we used v.1 downscaling realization to reduce intermodel variabilities of velocity estimates. Only the highest (RCP 8.5) and lowest (RCP 2.6) emissions scenarios satisfied these criteria. These criteria further omitted portions of the Arctic region due to differences in data resolutions across GCMs for these regions. To process CORDEX, we converted monthly climate values to annual mean temperature and total annual precipitation. We refer hereafter to these variables as 'temperature' and 'precipitation', respectively. We chose these variables because of their acknowledged importance in defining climate space for species[8,28]. Nevertheless, we acknowledge that different climate variables may also facilitate understanding ecosystem dynamics and global environmental change.

To examine the degree of instability species may face when relocating to track suitable climate analogues[13], we use the Land use Harmonization (LUH2) datasets[18]. LUH2 is a new generation of harmonization that builds on past work from CMIP5 at higher spatial resolution. We consider LUH2 v.2f, which uses harmonized land-use forcings for our study, which transitioned continuously from ReMIND-MAgPIE using new CMIP6 future scenarios (RCP 8.5/SSP 5). LUH2 v.2f contains annual states as a percentage of a 0.25°×0.25° degree grid. LUH2 also includes separating primary forest and secondary natural vegetation into the forest and non-forest subtypes, pasture into managed pasture and rangeland and cropland into multiple crop functional types. Therefore, we consider six major land-use states, including cropland (all functional groups), rangeland, managed pasture, primary forest, potentially forested secondary land and urban (Supplementary Table 4).

**Calculations of velocity of change.** Velocity of change measures the rate at which climate or land-use is displacing yearly (km yr$^{-1}$)[19,48]. To estimate velocity of climate change, we applied the VoCC in the R statistical computing platform (v.4.0.2)[49]. Traditionally, VoCC features two approaches—distance- and gradient-based (dVoCC and gVoCC). For model runs, gVoCC divides a linear slope (°C yr$^{-1}$, mm yr$^{-1}$ or % yr$^{-1}$) for each epoch by the spatial gradient (°C km$^{-1}$, mm km$^{-1}$ or % km$^{-1}$). Linear slopes of temperature and precipitation were coefficients extracted using simple ordinary least squares over 30 yr. The spatial gradient is a vector sum of longitudinal and latitudinal pairwise differences in temperature or precipitation at each focal cell using a 3×3 cell neighbourhood. We averaged velocity estimates between GCMs for the same variable within an RCP scenario to produce an ensemble estimate. We define 'climate velocity' as the absolute sum of precipitation and temperature velocities. We applied the same modelling approach to the ten land-use types. Unlike climate, land-use instability is defined as absolute sum of ten land-use typologies, spanning primary forest, secondary forests, cropland (five classes), pasture, rangeland and urban.

**Risks assessment.** We examined the exposure risk of global terrestrial PAs by merging multivariate metrics into an exposure space bounded by climate velocity and land-use instability during the near future (2021–2050). Each axis was scaled relative to the global median of the baseline epoch. We used PA polygons from the 2021 World Database on Protected Areas (WDPA)[50] datasets (except for China, where we used the 2016 WDPA polygons as these PAs are excluded from the 2021 version). We performed spatial-data cleaning in ESRI ArcGIS 10.6.1 by applying quality filters outlined in the Supplementary Information. Using a cell centre coverage algorithm, we rasterized the polygons to the spatial resolution of CORDEX. Our selected PAs made up ~18×10$^6$ km$^2$ (Supplementary Table 4) or ~14% of the terrestrial area evaluated. Of these, ~20% (~3.6×10$^6$ km$^2$) were within IUCN management categories I–II (which we refer to as strict management).

Finally, we examine the relationship between four characteristics of PAs (richness of tetrapods and vascular plants, elevation, distance from coasts and IUCN management category) and climate velocity and land-use instability. Systematic monitoring across all important sites (to determine whether the current management regime effectively retains or restores a site's biodiversity value) is required to achieve post-2020 biodiversity conservation objectives[51]. To this end, we represent relative conservation values of PAs by extracting species richness. Thus, we built equal-area grids (24 km grain size) and overlaid with expert-derived extent-of-occurrence range maps for terrestrial birds (10,830 species), mammals (5,654 species), reptiles (7,105 species), amphibians (6,615 species) and modelled native richness of vascular plants. For tetrapods, we considered species designated as extant, native and either breeding or resident. Thus, we assess whether PAs important for the conservation of species are disproportionately impacted by projected climate and land-use changes. To represent how topographic heterogeneity may become an impediment to migrating species as climate change intensifies[29] or may buffer against climate-induced biodiversity loss, we used the shuttle radar topography mission's digital elevation model (STRM-DEM)[52]. To examine how a sharp coastal climate gradient might influence potential species migration[28], we quantified distance from the ocean. Additionally, from a land use and ecological standpoint, projected coastal development by 2100 may increase pressure on PAs and global conservation goals. Distance from the coast was defined as the Euclidean distance (km) using a boundary shapefile retrieved from GADM v.3.4 (www.gadm.org) and was implemented in ESRI ArcGIS v.10.6.1. Analyses were repeated across 14 biomes using a shapefile obtained from the Worldwide Fund for Nature (WWF) database[53].

**Reporting Summary.** Further information on research design is available in the Nature Research Reporting Summary linked to this article.

## Data availability

All underlying raw model data are publicly available online. CORDEX climate data are available at https://esgf-data.dkrz.de/search/cmip5-dkrz/. Land-use Harmonization data are available at https://luh.umd.edu/data.shtml. WDPA is freely available online at Protected Planet Network https://www.protectedplanet.net/en/thematic-areas/wdpa?tab=WDPA. Expert-derived polygons of amphibians, mammals and reptiles are available online at the IUCN Red List Portal https://www.iucnredlist.org/resources/spatial-data-download. Polygons of birds' distributions can be requested from BirdLife International http://datazone.birdlife.org/species/requestdis. Datasets on native richness of vascular plants were obtained from ref. [54]. Biomes and ecoregional polygons are available at WWF database https://www.worldwildlife.org/publications/terrestrial-ecoregions-of-the-world. Map elements: (1) bounding box ('ne_110m_wgs84_bounding_box' layer) can be downloaded from Natural Earth database https://www.naturalearthdata.com/ and (2) Land border was retrieved using the getMap() function of rworldmap library in R. Climate (temperature and precipitation) and land-use (cropland, primary forest, secondary forest, pasture, rangeland and urban) rasters for each period are available at Figshare (https://doi.org/10.6084/m9.figshare.14852955.v4)[55].

## Code availability

Authors calculated climate and land-use velocities using VoCC package of R statistical computing platform v.4.0.2 (ref. [49]). Codes for visualizations are available on Figshare (https://doi.org/10.6084/m9.figshare.14852955.v4)[55]. More information about the codes and data can be obtained from the corresponding author on request.

## References


45. Williams, K. D. et al. The Met Office Global Coupled model 2.0 (GC2) configuration. *Geosci. Model Dev.* **8**, 1509–1524 (2015).
46. Giorgetta, M. A. et al. Climate and carbon cycle changes from 1850 to 2100 in MPI-ESM simulations for the Coupled Model Intercomparison Project Phase 5. *J. Adv. Model. Earth Syst.* https://doi.org/10.1002/jame.20038 (2013).
47. Knudsen, E. M. & Walsh, J. E. Northern Hemisphere storminess in the Norwegian Earth System Model (NorESM1-M). *Geosci. Model Dev.* **9**, 2335–2355 (2016).
48. Brito-Morales, I. et al. Climate velocity can inform conservation in a warming world. *Trends Ecol. Evol.* **33**, 441–457 (2018).
49. García Molinos, J., Schoeman, D. S., Brown, C. J. & Burrows, M. T. VoCC: an R package for calculating the velocity of climate change and related climatic metrics. *Methods Ecol. Evol.* **10**, 2195–2202 (2019).
50. UNEP-WCMC & IUCN *Protected Planet: The World Database on Protected Areas* (WDPA, 2018).
51. Visconti, P. et al. Protected area targets post-2020. *Science* **364**, eaav6886 (2019).
52. Farr, T. G. et al. The shuttle radar topography mission. *Rev. Geophys.* https://doi.org/10.1029/2005RG000183 (2007).
53. Olson, D. M. et al. Terrestrial ecoregions of the world: a new map of life on Earth. *BioScience* **51**, 933–938 (2001).
54. Ellis, E. C., Antill, E. C. & Kreft, H. All is not loss: plant biodiversity in the anthropocene. *PLoS ONE* **7**, 30535 (2012).
55. Asamoah, E. F. *Climate Velocity and Land-use Instability 1971–2100* (Figshare, 2021); https://doi.org/10.6084/m9.figshare.14852955.v4


## Acknowledgements

We thank M. Di Marco for providing comments on an earlier version of this work. E.F.A. acknowledges PhD support from Macquarie University through the International Macquarie Research Excellence Scholarship (iMQRES) programme.

## Author contributions

E.F.A. and J.M.M. conceived the study. E.F.A. performed the analysis and led the manuscript with L.J.B. and J.M.M. All authors critically edited the manuscript.

## Competing interests

The authors declare no competing interests.

## Additional information

**Extended data** is available for this paper at https://doi.org/10.1038/s41558-021-01223-2.

**Supplementary information** The online version contains supplementary material available at https://doi.org/10.1038/s41558-021-01223-2.

**Correspondence and requests for materials** should be addressed to Ernest F. Asamoah.

**Peer review information** *Nature Climate Change* thanks Isabel Rosa and the other, anonymous, reviewer(s) for their contribution to the peer review of this work.

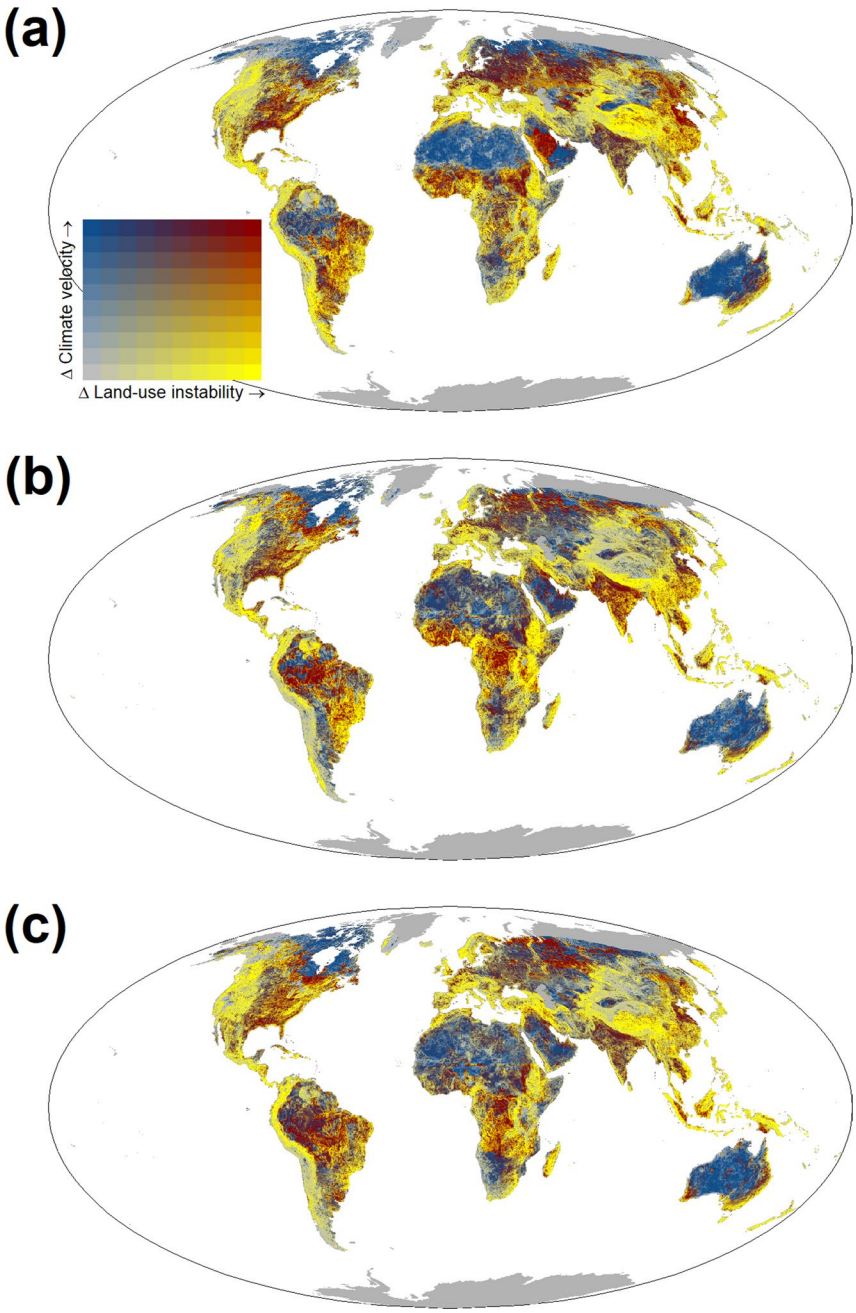


**Extended Data Fig. 1 | Global patterns of the combined climate change velocity and land-use instability.** (**a–c**) A bivariate choropleth of climate and land-use velocities showing two-dimensional velocity space across the globe during 1971–2000, 2021–2050 and 2071–2100 epochs. Climate velocity and land-use instability metrics were both reclassified into frequency distributions of percentile bins. Both climate and land-use change results are based on a spatial resolution of 24 km in a Mollweide projection (ESRI: 54009).

nature research

Corresponding author(s): Ernest Frimpong Asamoah

Last updated by author(s): Oct 15, 2021

# Reporting Summary

Nature Research wishes to improve the reproducibility of the work that we publish. This form provides structure for consistency and transparency in reporting. For further information on Nature Research policies, see our Editorial Policies and the Editorial Policy Checklist.

## Statistics

For all statistical analyses, confirm that the following items are present in the figure legend, table legend, main text, or Methods section.

| n/a | Confirmed | |
|---|---|---|
| ☐ | ☒ | The exact sample size (*n*) for each experimental group/condition, given as a discrete number and unit of measurement |
| ☒ | ☐ | A statement on whether measurements were taken from distinct samples or whether the same sample was measured repeatedly |
| ☐ | ☒ | The statistical test(s) used AND whether they are one- or two-sided<br>*Only common tests should be described solely by name; describe more complex techniques in the Methods section.* |
| ☒ | ☐ | A description of all covariates tested |
| ☐ | ☒ | A description of any assumptions or corrections, such as tests of normality and adjustment for multiple comparisons |
| ☐ | ☒ | A full description of the statistical parameters including central tendency (e.g. means) or other basic estimates (e.g. regression coefficient) AND variation (e.g. standard deviation) or associated estimates of uncertainty (e.g. confidence intervals) |
| ☐ | ☒ | For null hypothesis testing, the test statistic (e.g. *F*, *t*, *r*) with confidence intervals, effect sizes, degrees of freedom and *P* value noted<br>*Give P values as exact values whenever suitable.* |
| ☒ | ☐ | For Bayesian analysis, information on the choice of priors and Markov chain Monte Carlo settings |
| ☒ | ☐ | For hierarchical and complex designs, identification of the appropriate level for tests and full reporting of outcomes |
| ☐ | ☒ | Estimates of effect sizes (e.g. Cohen's *d*, Pearson's *r*), indicating how they were calculated |

*Our web collection on statistics for biologists contains articles on many of the points above.*

## Software and code

Policy information about availability of computer code

| | |
|---|---|
| Data collection | CORDEX climate data used are available at https://esgf-data.dkrz.de/search/cmip5-dkrz/. Land-use Harmonisation data used are available here (https://luh.umd.edu/data.shtml) |
| Data analysis | We used VoCC package of R version 4.0.2, ArcGIS 10.6.1 (student license). Datasets and codes are available on Figshare (https://doi.org/10.6084/m9.figshare.14852955.v3). |

For manuscripts utilizing custom algorithms or software that are central to the research but not yet described in published literature, software must be made available to editors and reviewers. We strongly encourage code deposition in a community repository (e.g. GitHub). See the Nature Research guidelines for submitting code & software for further information.

## Data

Policy information about availability of data

All manuscripts must include a data availability statement. This statement should provide the following information, where applicable:

- Accession codes, unique identifiers, or web links for publicly available datasets
- A list of figures that have associated raw data
- A description of any restrictions on data availability

CORDEX climate data used are available at https://esgf-data.dkrz.de/search/cmip5-dkrz/. Land-use Harmonisation data used are available here (https://luh.umd.edu/data.shtml), Polygons of protected are boundaries are available at https://www.protectedplanet.net/en/thematic-areas/wdpa?tab=WDPA. Mammal, reptile, and amphibian species distribution maps are available online (https://www.iucnredlist.org/resources/spatial-data-download). Polygons of birds' distributions can be requested from BirdLife International (http://datazone.birdlife.org/species/requestdis). Polygons of biomes and ecoregions are available at WWF database (https://www.worldwildlife.org/publications/terrestrial-ecoregions-of-the-world). Map elements, such as bounding box and land borders ca =n be retrieved from Natural Earth database (https://www.naturalearthdata.com/) and using getMap() function of rworldmap library in R, respectively. Model outputs,

including climate (temperature and precipitation) and land-use (cropland, primary forest, secondary forest, pasture, rangeland, and urban) rasters for each period,are available at Figshare under the identifier https://doi.org/10.6084/m9.figshare.14852955.v3)

# Field-specific reporting

Please select the one below that is the best fit for your research. If you are not sure, read the appropriate sections before making your selection.

☐ Life sciences ☐ Behavioural & social sciences ☒ Ecological, evolutionary & environmental sciences

For a reference copy of the document with all sections, see nature.com/documents/nr-reporting-summary-flat.pdf

# Ecological, evolutionary & environmental sciences study design

All studies must disclose on these points even when the disclosure is negative.

| | |
|---|---|
| Study description | We sought to understand whether climate change and land-use driven habitat loss interact synergistically to undermine potential benefits of protected areas including the conservation and restoration of global biodiversity. We calculated velocity as the quotient of long-term trend to spatial gradient. |
| Research sample | This study used existing datasets. For climate, we use monthly temperature and precipitation layers from Coordinated Regional Climate Downscaling Experiment (CORDEX) [ref 17 in main text], predicted under scenario RCP2.6 and RCP8.5. For both of these climate variables, we use three global circulation models (GCMs), MOHC-HadGEM2-ES, MPI-M-MPI-ESM-LR and NCC-NorESM1-M. All climate data were version one downscaling realisation. Land-use data (10 typologies) were downloaded from the Land Use Harmonisation website (ref 18 in main text). |
| Sampling strategy | We used 10 CORDEX domains for both temperature and precipitation variables |
| Data collection | Modelled temperature, precipitation and land-use data (ten LU classes) were used in this study. |
| Timing and spatial scale | All data were retrieved from online repositories accessed during the period January/2020-December/2020. Estimate of climate and land-use instabilities were conducted across three epochs: 1971-2000, 2021-2050 and 2071-2100 at yearly resolution, on a 0.22 degree grid. Summaries are provided for biomes, ecoregions, and across protected areas. |
| Data exclusions | Data were not excluded from analysis |
| Reproducibility | All data is openly available |
| Randomization | Not relevant. |
| Blinding | Not relevant. |

Did the study involve field work? ☐ Yes ☒ No

# Reporting for specific materials, systems and methods

We require information from authors about some types of materials, experimental systems and methods used in many studies. Here, indicate whether each material, system or method listed is relevant to your study. If you are not sure if a list item applies to your research, read the appropriate section before selecting a response.

## Materials & experimental systems

| n/a | Involved in the study |
|---|---|
| ☒ | ☐ Antibodies |
| ☒ | ☐ Eukaryotic cell lines |
| ☒ | ☐ Palaeontology and archaeology |
| ☒ | ☐ Animals and other organisms |
| ☒ | ☐ Human research participants |
| ☒ | ☐ Clinical data |
| ☒ | ☐ Dual use research of concern |

## Methods

| n/a | Involved in the study |
|---|---|
| ☒ | ☐ ChIP-seq |
| ☒ | ☐ Flow cytometry |
| ☒ | ☐ MRI-based neuroimaging |